The controlled charge ordering and evidence of the metallic state in $Pr_{0.65}Ca_{0.35}MnO_3$ films

2000 J. Phys.: Condens. Matter 12 L133

(http://iopscience.iop.org/0953-8984/12/6/112)

J. Phys.: Condens. Matter **12** (2000) L133–L138. Printed in the UK PII: S0953-8984(00)08730-0

LETTER TO THE EDITOR

The controlled charge ordering and evidence of the metallic state in $Pr_{0.65}Ca_{0.35}MnO_3$ films

Y P Lee†, V G Prokhorov†‡, J Y Rhee§, K W Kim†, G G Kaminsky‡ and V S Flis‡

† Department of Physics, Sunmoon University, Asan, Choongnam, 336-840, Korea
‡ Institute of Metal Physics, National Academy of Sciences of Ukraine, Kiev, 252142, Ukraine
§ Department of Physics, Hoseo University, Asan, Choongnam, 336-795, Korea

Received 14 October 1999, in final form 15 December 1999

Abstract. The resistivity of $Pr_{0.65}Ca_{0.35}MnO_3$ films prepared by pulsed laser deposition has been measured in the temperature range 4.2–300 K. The formation of metallic phase is suggested by the analysis of the temperature dependence of resistivity at low temperatures under zero-magnetic field. It is shown that the appearance of the charge-ordered state at 205 K can be controlled by the lattice strains accumulated during the film growth. The charge-ordering energy gap was estimated to be 77.5 meV from the experimental data. Experimental results are interpreted on the basis of the phase-separation model.

The $Pr_{0.65}Ca_{0.35}MnO_3$ compound belongs to a family of perovskite-like manganites $R_{1-x}A_xMnO_3$ (R = La, Nd or Pr, and A = Ca, Ba or Sr) which shows the colossal magnetoresistance (CMR) phenomenon [1, 2]. The magnetic and electronic properties of the CMR compounds have traditionally been explained by the double exchange (DE) model [3] which considers the transfer of an electron (or hole) between neighbouring Mn^{3+} and Mn^{4+} ions through the Mn–O–Mn chains. Another important feature of the manganites is closely related to a strong structural distortion interpreted in terms of the cooperative Jahn–Teller (JT) effect [4]. The orbital ordering resulting from the JT distortion leads to the possibility of the formation of two different states denoted as charge-ordered (CO) insulating, and charge-disordered (CD) or charge-delocalized metallic-like states in the compound [5, 6]. A strong correlation between structural and electronic states suggests that the physical properties of these compounds are very sensitive to the method of preparation and subsequent treatments. It will be shown that $Pr_{0.65}Ca_{0.35}MnO_3$ thin films display an incomplete transition into the metallic phase, while the bulk compound remains in the insulating phase at any temperature [7, 8]. In contrast to the Mott's variable-range hopping (VRH) model [9], or the well known thermally-activated conductivity (TAC) of the lattice (or magnetic) polarons [10, 11] we propose a new explanation for the exponential behaviour of resistivity which is based on the existence of small size (∼10–20 Å) ferromagnetic (FM) clusters in the paramagnetic (PM) matrix of the compound.

In this letter we report the experimental results of the resistivity for $Pr_{0.65}Ca_{0.35}MnO_3$ films prepared by a laser ablation method. Two Nd-YAG lasers with a wavelength of 1064 nm, a pulse duration of 7.8–10.5 ns and an energy of 0.3 J/pulse were used. The pulse repetition rate was 20 Hz. The power density of the laser beam focused on the target was 9.5×10^8–2×10^{10} W cm^2. A cross-beam deposition scheme utilizing the two lasers was employed to

0953-8984/00/060133+06$30.00

avoid hitting the substrate with large-size particles from the target [12]. For the preparation of the $Pr_{0.65}Ca_{0.35}MnO_3$ target, first, Pr_6O_{11}, CaO and Mn_2O_3 powders were mixed in proportion to the stoichiometric composition and then annealed at 1000 °C for three days in air. The cooled powders were then hot-pressed and heated at 1200 °C for four days to manufacture the targets. X-ray diffraction (XRD) analyses revealed that the lattice constants of the targets ($a = 5.42$ Å; $b = 5.45$ Å; $c = 7.67$ Å) correspond to the stoichiometric $Pr_{0.65}$ $Ca_{0.35}MnO_3$ compound [13]. The substrate was a $LaAlO_3$ (100) single crystal with a lattice parameter $a = 3.82$ Å for pseudocubic symmetry. The substrate temperature during deposition was 750 °C. The oxygen pressure in the chamber was maintained at 200 Torr during deposition and at 600 Torr during cooling after deposition. Under these conditions $Pr_{0.65}Ca_{0.35}MnO_3$ films were obtained with a thickness (d) of about 2000 Å. In some cases the films were annealed at 900 °C for 1–10 h in air.

The θ–2θ XRD patterns were obtained using a Rigaku diffractometer with Cu-K_α radiation. A small angle of scanning (0.024°) allows us to estimate accurately the full width at half maximum (FWHM) of the large-angle peaks. The lattice parameters evaluated directly from the XRD data were plotted against $\cos^2\theta/\sin\theta$. By fitting the extrapolated straight line to $\cos^2\theta/\sin\theta = 0$, a more precise determination of the lattice parameter is possible [14]. The resistance was measured by using the four-point-probe method in a temperature range of 4.2–300 K.

Figure 1 presents the θ–2θ XRD scans of the (a) as-deposited and (b) annealed (at 900 °C for 2 h) $Pr_{0.65}Ca_{0.35}MnO_3$ films. Only the (00l) peaks of the substrate and film are significantly manifested, indicating that the deposition results in a highly oriented film. On the other hand,

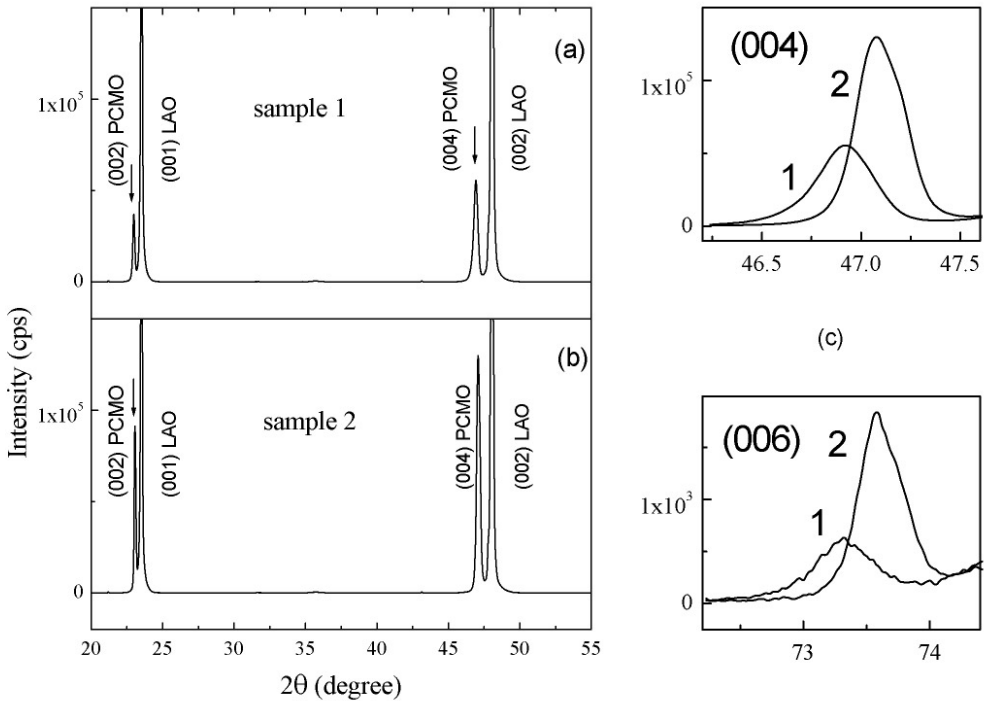

Figure 1. $\theta - 2\theta$ XRD patterns of the (a) as-deposited and (b) annealed $Pr_{0.65}Ca_{0.35}MnO_3$ films. (c) The (004) and (006) difraction peaks of the as-deposited ('1') and annealed ('2') films.

the presence of small peaks for the (103), (113) and (312) reflections allows us to calculate the lattice parameters for the films. In contrast to the bulk compound [13], the deposited films have a tetragonal rather than orthorhombic crystal structure with the following lattice parameters: $a \simeq b = 5.432$ Å and $c = 7.74$ Å, and $a \simeq b = 5.551$ Å and $c = 7.719$ Å for the as-deposited and annealed films, respectively. This can be explained by an essential influence of the substrate on the crystal structure and the lattice distortion of the film. Note that the values of a and b for the as-deposited film are very close to $a\sqrt{2} \simeq 5.401$ Å of the substrate. Figure 1(c) shows that annealing of the film results not only in a shift of the peak position, but in a narrowing of peak width. For the as-deposited (annealed) film the FWHM is 0.323° (0.262°) and 0.563° (0.41°) for the (004) and (006) reflections, respectively. Consequently, one can consider that uniform and nonuniform lattice strains are accumulated during the film growth and most of them are relaxed by the high-temperature annealing. It was also observed that the oxygen diffusion in the film began if the annealing time was longer than 10 h. This was shown by the opposite shift of (00l) peak positions and the increased lattice parameter c.

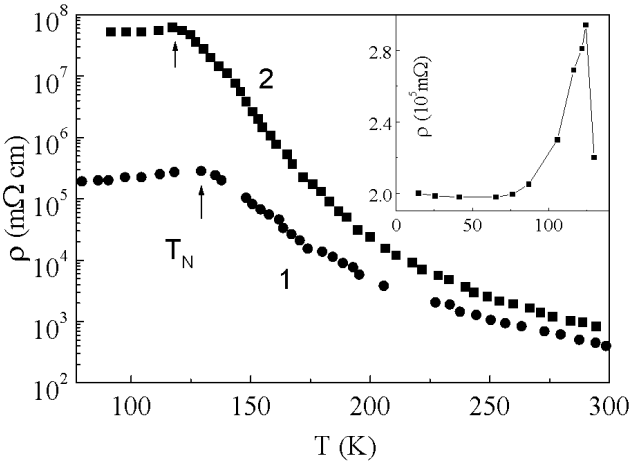

Figure 2. Temperature dependence of the resistivity for the as-deposited ('1') and annealed ('2') $Pr_{0.65}$ $Ca_{0.35}MnO_3$ films. The inset displays the metallic-like behaviour of $\rho(T)$ below T_N for the as-deposited film.

Figure 2 shows the temperature dependence of resistivity, $\rho(T)$, for the as-deposited and annealed films. It is seen that, down to Néel temperature T_N ($\approx$ 130 K [13]), $\rho(T)$ of the films exhibits an exponential behaviour. However, in the low temperature range ($T < T_N$) an abrupt change is observed in $\rho(T)$, which can be interpreted as an appearance of metallic phase. The inset of figure 2 shows $\rho(T)$ of the as-deposited film below T_N. Although a complete transition into metallic phase is not seen, a forerunner of such a conversion is observed distinctly. The observed difference in the transport properties between bulk [7, 8] and thin-film $Pr_{0.65}Ca_{0.35}MnO_3$ compounds can be connected with an essential distortion of the MnO_6 octahedra in the epitaxial films. It was shown that, in $La_{1-x}Sr_xMnO_3$, a larger Mn–O–Mn angle in the rhombohedral phase results in the tendency of the insulator–metal transition [15]. In figure 2, the annealed film exhibits an enhanced resistivity in the whole temperature range and a shift of resistivity maximum temperature near T_N by 10 K to lower side. Therefore, the $\rho(T)$ behaviour of the annealed film becomes close to that of the bulk materials.

The exponential behaviour of the resistivity may be explained in terms of the VRH

model [9], or by TAC of lattice (or magnetic) polarons [10, 11]. The VRH expression for the resistivity is written as $\rho(T) = \rho_\infty \exp[(T_0/T)^{1/4}]$, where ρ_∞ is the resistivity at $T = \infty$, and T_0 is the localization energy of carriers in units of temperature. On the other hand, the TAC expression of resistivity can be written in the Arrhenius form: $\rho(T) = \rho_0 T \exp(T_a/T)$, where T_a is the activation energy in units of temperature. The best agreement between the experimental and theoretical curves for the as-deposited films is seen with the fitting parameters of $\rho_\infty \lesssim 10^{-13}$ mΩ cm and $T_0 = 4.4 \times 10^8$ K for the VRH model, and $\rho_0 = 3 \times 10^{-3}$ mΩ cm K^{-1} and $T_a = 1800$ K for the TAC model.

The value of T_0 in the VRH model depends on the electron localization length, ℓ_0, and the electron density of states at the Fermi level, $N(E_F)$; $k_B T_0 = 18/[\ell_0^3 N(E_F)]$ [16]. Using the e_g band width of $E_B \approx 0.3$ eV [17] and the estimated carrier concentration of $n \approx 1.87 \times 10^{21}$ cm^{-3}, one can obtain $\ell_0 = 2.3 \times 10^{-6}$ Å which is far from any physical sense. It should be noted that such an unrealistically small value of ℓ_0 is usually obtained in the resistance analysis of other perovskite-like manganites [8, 16–18].

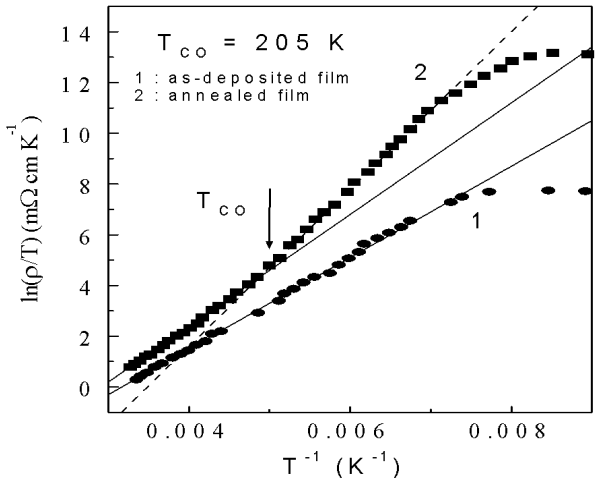

Figure 3. $\ln(\rho/T)$ against T^{-1} for $Pr_{0.65}Ca_{0.35}MnO_3$ film before ('1') and after ('2') an annealing. The charge-ordering temperature T_{CO} for this compound $\simeq$ 205 K.

Figure 3 shows the $\ln(\rho/T)$ against T^{-1} plots for the film before and after annealing. The plot for the as-deposited film can be described in terms of a single theoretical straight line with aforementioned fitting parameters of the TAC model. However, for the annealed film, there are two linear ranges with different values for the fitting parameters (the solid and dashed lines for data 2 in figure 3) of $T_a = 3100$ K and $\rho_0 = 2.04 \times 10^{-5}$ mΩ cm K^{-1} at low temperature, and $T_a = 2200$ K and $\rho_0 = 1.66 \times 10^{-3}$ mΩ cm K^{-1} at high temperature [19]. The temperature of the kink ($\simeq$ 205 K), at which the slope of $\ln(\rho/T)$ against T^{-1} changes, corresponds to the charge-ordering-transition temperature (T_{CO}) [7, 20, 21]. Consequently, it can be concluded that the CO state (a real-space ordering of the Mn^{3+} and Mn^{4+} ions) leads to the enhancement of the activation energy of carriers, and the activation energy difference or charge-ordering energy gap between the CO and CD states is $\Delta_{CO} \approx 900$ K or 77.5 meV. A similar value of energy gap in the CO insulating phase was obtained for the $Pr_{0.5}Sr_{0.5}MnO_3$ compound by photoemission spectroscopy [22]. Although physical peculiarities of the CO state have been investigated very intensively in recent years, the nature of this effect is still a matter of speculation. Most of the experimental results can be summarized as follows: the CO transition is accompanied by a lattice distortion and a volume increase [7, 8, 21, 23], the

application of a magnetic field results in the melting of the CO state [7, 23–25], and the CO state is suppressed by applying a pressure [26] or illuminating an x-ray [27].

The results of our work clearly show that the charge-ordering transition can be controlled by lattice strains. Owing to a lattice mismatch between substrate and film, the as-deposited films are significantly strained (see figure 1(c)). These lattice strains might obstruct the CO in the as-deposited films, while annealing at a high temperature would result in a relaxation of the strains and thus in the CO transition at $T_{CO} \simeq 205$ K.

The TAC behaviour for the manganese oxides is more intensively examined on the basis of diffusive motion of the small lattice polarons (Holstein polarons) whose dimension is comparable to the lattice parameter [1, 5, 11, 16, 28]. In this case, any small lattice distortion of the JT kind can lead to a localization of polarons and the TAC mechanism. In the adiabatic limit, $\rho_0 = k_B/(n_p e^2 \omega_{op} a_p^2)$, where a_p is the hopping distance of polarons, n_p is the polaron concentration determined by the number of the divalent cations, and ω_{op} is the optical phonon frequency. Using $\omega_{op} \approx 10^{14}$ s^{-1} [29] and the polaron concentration, which is equal to the hole concentration (concentration of the Ca^{2+} ions), one can estimate the polaron hopping distance from the fitted value of ρ_0. It turns out to be $a_p \approx 3.1$ Å which practically coincides with the crystal lattice parameter. The activation energy consists of two terms, $T_a = E_g/2 + W_H$, where W_H is the polaron formation energy and E_g is the so-called trapping energy or the energy difference between lattice distortions with and without hole [30]. If it is assumed that the polaron formation energy is equal to the e_g-band width, and $E_g \ll W_H$ as a rule [11, 23, 31], one can estimate the polaron radius according to reference [29]. The estimated value is about 9.7 Å and is larger than the hopping distance. Therefore, it is hard to say that the polaron moves via a hopping mechanism. Rather, its motion is more likely to be a creep-like behaviour of the local lattice deformations. Since the high level of lattice distortion in the overstrained as-deposited film naturally induces an increase in the polaron-trapping energy, the value of T_a must be higher for the as-deposited film than the annealed one in the framework of polaron model for conductivity. However, this is not the case for our experimental data (see figure 3).

The charge-ordering energy gap is closely related to the change in the electronic band structure, due to the e_g-orbital ordering and the distortion of the MnO_6 octahedron [2]. Therefore, another scenario can be considered for the explanation of the experimental results. The observation of the small-size FM clusters by neutron scattering within the PM matrix of $La_{0.67}Ca_{0.33}MnO_3$ is direct experimental evidence that a dynamic phase separation can occur in real materials [24, 32]. The FM clusters can be treated as potential wells for electrons and holes because they have an unsplit wide d band near the Fermi level [2]. In the PM surroundings, owing to the Mott–Hubbard interactions, the d band of the transition metal splits into the upper and lower Hubbard bands, resulting in an energy gap between the two Hubbard bands. Outside the clusters the transport can be explained in terms of the TAC mechanism, where the activation energy is defined as the difference between the lower edge of the upper Hubbard band (in the PM matrix) and the Fermi level (in the FM cluster). The small size of the FM clusters allows us to consider them as electron (or hole) traps with an energy state lower than the surrounding. The transition to the CO state for the annealed film leads to a decrease of bandwidth of the two Hubbard bands and thus to an increase in the activation energy. At temperatures below the magnetic transition the fluctuated FM clusters, under the action of an intrinsic magnetic field, coalesce into larger FM domains which cannot play a role as one-particle traps and form a percolation net of metallic-like conductive channels into the dielectric matrix. This process, in turn, results in the frustration of the TAC mechanism (see figure 2) and the exponential behaviour of the resistivity terminates at $T \approx T_N$. The incomplete transition to the metallic-like phase is probably due to an insufficient volume of ferromagnetically aligned phase in our films.

In summary, the effect of lattice strains on the transport properties of $Pr_{0.65}Ca_{0.35}MnO_3$ films has been investigated. In contrast to the bulk compound, $\rho(T)$ changes abruptly near T_N, below which the resistivity follows a metallic-like behaviour. The charge ordering observed at $T = 205$ K can be controlled by lattice strains accumulated during the film growth. The TAC model is more suitable for describing the temperature dependence of resistance for the $Pr_{0.65}Ca_{0.35}MnO_3$ films in the high temperature range than the VRH conductivity. The observed experimental results and the metallic-like behaviour at low temperature were also explained by the phase-separation model.

This work was supported by the Korea Science and Engineering Foundation through the Atomic-scale Surface Science Research Center and through Project Nos 97-0702-01-01-3 and 995-0200-004-2 and also by Korea Research Foundation Grant (KRF-99-D00048).

References

[1] Ramirez A P 1997 *J. Phys.: Condens. Matter* **9** 8171
[2] Khomskii D I and Sawatzky G A 1997 *Solid State Commun.* **102** 87
[3] Zener C 1951 *Phys. Rev.* **82** 403; Anderson P W and Hasegawa H 1955 *Phys. Rev.* **100** 675
[4] Millis A J, Littlewood P B and Shraiman B I 1995 *Phys. Rev. Lett.* **74** 5144
[5] Schiffer P, Ramirez A P, Bao W and Cheong S-W 1995 *Phys. Rev. Lett.* **75** 3336
[6] Urushibara A, Maritomo Y, Arima T, Asamitsu A, Kido G and Tokura Y 1995 *Phys. Rev.* itB **51** 14103
[7] Yoshizawa H, Kawano H, Tomioka Y and Tokura Y 1995 *Phys. Rev.* itB **52** R13145
[8] De Teresa J M, Ibarra M R, Marquina C, Algarabel P A and Oseroff S 1996 *Phys. Rev.* B **54** R12689
[9] Mott N F 1990 *Metal-Insulator Transitions* 2nd edn (London: Taylor and Francis)
[10] Emin D and Holstein T 1969 *Ann. Phys., Lpz.* **53** 439
[11] Iguchi E, Ueda K and Jung W 1996 *Phys. Rev.* B **54** 17431
[12] Prokhorov V G, Matsui V I and Vas'ko V A 1992 *Superconductivity: Phys. Chem. Technol.* **6** 505 (Russian)
[13] Jirák Z, Krupička S, Šimša Z, Dlouhá M and Vratislav S 1985 *J. Magn. Magn. Mater.* **53** 153
[14] Bhatt H D, Vedula R, Desu S B and Fralick G C 1999 *Thin Solid Films* **350** 249
[15] Mitchel J F, Argyriou D N, Potter C D, Hinks D G, Jorgensen J D and Bader S D 1996 *Phys. Rev.* B **54** 6172
[16] Viret M, Ranno L and Coey J M D 1997 *Phys. Rev.* B **55** 8067
[17] Viret M, Ranno L and Coey J M D 1997 *J. Appl. Phys.* **81** 4964
[18] Blamire M G, Teo B-S, Durrell J H, Mathur N D, Barber Z H, Drissoll J L M, Cohen L F and Evetts J H 1999 *J. Magn. Magn. Mater.* **191** 359
[19] The experimental values of activation energy are very close to the optical gap of $Pr_{0.6}Ca_{0.4}MnO_3$ single crystal estimated in reference [29].
[20] Shen S-Q and Wang Z D 1998 *Phys. Rev.* B **58** R8877
[21] Tomioka Y, Asamitsu A, Kuwahara H, Moritomo Y and Tokura Y 1996 *Phys. Rev.* B **53** R1689
[22] Chainani A, Kumigashira H, Takahashi T, Tomioka Y, Kuwahara H and Tokura Y 1997 *Phys. Rev.* B **56** R15513
[23] Lees M R, Barratt J, Balakrishnan G and Paul D M 1995 *Phys. Rev.* B **52** R14303
[24] De Teresa J M, Ibarra M R, Algarabel P A, Ritter C, Marquina C, Blasco J, García J, del Moral A and Arnold Z 1997 *Nature* **386** 256
[25] Okimoto Y, Tomioka Y, Onose Y, Otsuka Y and Tokura Y 1998 *Phys. Rev.* B **57** R9377
[26] Yoshizawa H, Kajimoto R, Kawano H, Tomioka Y and Tokura Y 1997 *Phys. Rev.* B **55** 2729
[27] Kiryukhin V, Casa D, Hill J P, Keimer B, Vigliante A, Tomioka Y and Tokura Y 1997 *Nature* **386** 813
[28] Radaelli P G, Cox D E, Marezio M and Cheong S-W 1997 *Phys. Rev.* B **55** 3015
[29] Jaime M, Salamon M, Rubinstein M, Treece R, Horwitz J and Chriey D 1996 *Phys. Rev.* B **54** 11914
[30] Iguchi E, Ueda K and Nakatsuga H 1998 *J. Phys.: Condens. Matter* **10** 8999
[31] Okimoto Y, Tomioka Y, Onose Y, Otsuka Y and Tokura Y 1998 *Phys. Rev.* B **57** R9377
[32] Goodenough J B and Zhou J-S 1997 *Nature* **386** 229